Biomaterials 34 (2013) 841–853

Contents lists available at SciVerse ScienceDirect

Biomaterials

journal homepage: www.elsevier.com/locate/biomaterials

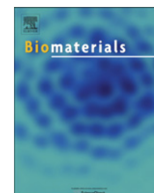

The spatial and temporal control of cell migration by nanoporous surfaces through the regulation of ERK and integrins in fibroblasts

Hsu-An Pan [a,1], Jia-You Liang [a,1], Yao-Ching Hung [b,c], Chia-Hui Lee [a], Jin-Chern Chiou [d], G. Steven Huang [a,*]

[a] Department of Materials Science and Engineering, National Chiao Tung University, Hsinchu 300, Taiwan, ROC
[b] College of Medicine, China Medical University, Taichung 40402, Taiwan, ROC
[c] Department of Obstetrics and Gynecology, China Medical University Hospital, Taichung 40402, Taiwan, ROC
[d] Institute of Electrical Control Engineering, National Chiao Tung University, Hsinchu 300, Taiwan, ROC

A R T I C L E I N F O

Article history:
Received 17 July 2012
Accepted 29 September 2012
Available online 3 November 2012

Keywords:
Nanopores
Stainless steel
Cell migration
Focal adhesion
Integrins
ERK

A B S T R A C T

Nanotopography controls cell behaviours, such as cell adhesion and migration. However, the mechanisms responsible for topology-mediated cellular functions are not fully understood. A variety of nanopores was fabricated on 316L stainless steel to investigate the effects of spatial control on the growth and function of fibroblasts, the temporal regulation of integrins, and their effects on migration. The NIH-3T3 fibroblast cell line was cultured on the nanopore surfaces, whose pore diameters ranged from 40 to 210 nm. The 40 and 75 nm nanopores enhanced cell proliferation, focal adhesion formation and protein expression of vinculin and β-tubulin after 24 h of incubation. Integrin expression was analysed by qPCR, which showed the extent of spatial and temporal regulation achieved by the nanopores. The protein expression of pERK1/2 was greatly attenuated in cells grown on 185 and 210 nm nanopore surfaces at 12 and 24 h. In summary, the 40 and 75 nm nanopore surfaces promoted cell adhesion and migration in fibroblasts by controlling the temporal expression of integrins and ERK1/2. The current study provides insight into the improvement of the design of stainless steel implants and parameters that affect biocompatibility. The ability to regulate the expression of integrin and ERK1/2 using nanopore surfaces could lead to further applications of surface modification in the fields of biomaterials science and tissue engineering.

© 2012 Elsevier Ltd. All rights reserved.

1. Introduction

Cell migration plays a critical role in a variety of biological and disease processes such as the healing of skin, connective tissue repair and inflammation [1]. After tissue injury, fibroblasts migrate towards the wound, enhance cell division near the edge of the wound and secrete ECM to support further cell migration [2]. The presence of various types of fibroblasts is critical to wound recovery [3]. Therefore, controlling fibroblast migration and proliferation is essential to improving tissue repair processes after implantation. The mechanics of cell migration are ascribed to the focal adhesion between integrin and ECM. The fibronectin receptor α5β1 integrin is highly expressed in human fibroblasts and promotes fibroblast motility and survival [4]. Moreover, α11β1 is the major receptor for collagen I on mouse embryonic fibroblasts and might be required for cell migration [5]. The optimum speed of cell migration occurs at intermediate levels of expression of α5β1 or α2β1 integrins or intermediate concentrations of ligands, including fibronectin or collagen [6]. In addition, the activation of the extracellular signal-regulated kinase (ERK) is believed to direct cell migration, attachment and integrins expression [7]. Studies have shown that integrin α2 plays a critical role in mediating ERK activation for cell adhesion and motility [8]. ERK is activated during the formation of focal adhesions and the regulation of human corneal epithelial cell migration associated with wound closure [9].

The ability of cells to adhere, migrate and express cell functions on metallic surfaces is crucial for tissue repair after implantation. One of the prevailing metallic materials is 316L stainless steel because its favourable combination of strength, fabrication properties and low *in vivo* toxicity make it suitable for use in orthopaedic, dental and surgical implants [10]. Further, 316L stainless steel shows reduced cytotoxicity and inflammatory response through the regulation of lactate dehydrogenase activity and

* Corresponding author. Department of Materials Science and Engineering, National Chiao Tung University, 1001 University Road, EE137, Hsinchu 300, Taiwan, ROC. Tel.: +886 3 5131451; fax: +886 3 5729912.
E-mail address: gstevehuang@mail.nctu.edu.tw (G.S. Huang).
[1] These authors contributed equally to this work.

0142-9612/$ – see front matter © 2012 Elsevier Ltd. All rights reserved.
http://dx.doi.org/10.1016/j.biomaterials.2012.09.078

tumour necrosis factor alpha in human monocytes [11]. Therefore, stainless steel can provide an anti-corrosion and non-cytotoxic surface to induce the adhesion of osteoblasts [12]. A critical factor to consider in developing metallic biomimetic cell-stimulating cues is the fact that the extracellular environment features nano-scale topographic interfaces. However, only a few studies have discussed the cellular responses of molecules such as integrin on metallic surface topographies. The focus of this study is to combine fundamental aspects of nanotopography and cellular molecular biology to temporally modulate cell-substrate responses between NIH-3T3 fibroblasts and nanopore surfaces of 316L stainless steel.

Surface modification has been used to improve the biocompatibility of stainless steel implants. Enhanced human osteoblast cell adhesion and proliferation has been observed on 316L stainless steel after calcium phosphate or hydroxyapatite-coated treatment [13]. However, hydroxyapatite and calcium phosphate coatings with thicknesses of ~10–100 μm are chemically unstable and exhibit deteriorating mechanical strength during long-term implantation *in vivo* [14,15]. Nanotopography may hold the key to modifying the surfaces and enhancing the mechanical strength of metallic implants. Previous studies have shown that the surfaces of 30 nm TiO_2 nanotubes promote stem cell adhesion, whereas nanotubes measuring 70–100 nm induce cytoskeletal stress and differentiation into osteoblast-like cells [16]. Endothelial cells are able to interact with 100 nm TiO_2 nanotubes to achieve enhanced cellular migration, focal adhesion and viability [17]. Furthermore, nanotopography may regulate integrins expression and modulate cell function. Structures featuring 14 nm deep pits enhance osteoblastic cell attachment and spreading by enhancing integrin αV expression [18]. Integrin α2β1 signalling, required for osteoblastic differentiation, can be induced by the sub-microstructure of the Ti surface [19]. Although the molecular mechanism that governs the topological control of nanostructures over cell migration is under intensive investigation, the temporal expression of genes in adapting to a nanostructured environment has yet to be explored. Furthermore, the correlation between the entire spectrum of integrins expression and cellular migration when interacting with nanostructured surfaces requires systematic investigation.

To further explore the general phenomenon of topological sensing, experiments using the NIH-3T3 cell line were performed to investigate the nanotopological influence of different nanoscale structures [20]. In the current study, nanopores with diameters ranging from 40 to 210 nm were created on stainless steel. The effects on cell growth, migration, and adhesion were evaluated. In particular, the temporal expression of integrins was quantified. The aim of this study was to investigate the size dependence of nanopore surfaces on the growth and function of fibroblasts and to discuss the interplay between adhesion and migration, together with advanced surface nano-engineering, which might help us understand cellular responses to nano-environments.

2. Materials and methods

2.1. Cell culture

To eliminate the possible contamination of nano-microparticles, cell culturing was performed in a class-10 clean room. NIH-3T3 fibroblasts were cultured in Dulbecco's Modified Eagle's Medium without antibiotics and were complimented with 10% FCS. The cells were incubated at 37 °C in 5% CO_2.

2.2. Chemicals

Glutaraldehyde and osmium tetroxide were purchased from Electron Microscopy Sciences (USA). Anti-vinculin mouse antibody was purchased from Abcam (USA). Alexa Fluor 594 phalloidin and Alexa Fluor 488 goat anti-mouse IgG were purchased from Invitrogen (USA). Trypsin was purchased from Sigma (USA). Bromodeoxyuridine and antibody were purchased from Millipore. Other chemicals of analytical grade or higher were purchased from Sigma or Merck. Anti-integrin rabbit antibody and anti-β-tubulin mouse antibody were purchased from Novus.

2.3. Fabrication of nanopore surfaces

Medical 316L stainless steel samples were mechanically polished with abrasive papers (grade 250, 800, 2000 and 4000) followed by alumina powder (0.3 μm). Electropolishing was then executed in an electrolytic bath, whose temperature was maintained between 5 and 10 °C for 30 min. The electrolyte was composed of a mixture of 40 mL of perchloric acid and 760 mL of ethylene-glycol monobutylether [21]. The applied voltages for anodisation were 30, 45, 60, 70, and 75 V for 40, 75, 160, 185, and 210 nm nanopore surfaces, respectively; the electrolytic solution was stirred by a rotating magnet. After electropolishing, the samples were rinsed with large amounts of distilled water and then cleaned with the electrolyte overnight. Polished stainless steel substrates were used as control flat substrates. Five flat nanopore surfaces ($n = 6$) were analysed by scanning electron microscopy (JEOL JSM-6500 TFE-SEM). Atomic force microscopy (AFM) was used to characterise the depths and roughness of the substrates.

2.4. Morphological observation by scanning electron microscopy (SEM)

Fibroblasts were seeded at a density of 5.0×10^3 cells/cm^2 on the different nanopore surfaces for 12, 24, 48 and 72 h of incubation. After removing the culture medium, the wells were rinsed three times with phosphate buffer saline (PBS). The cells were fixed with 1% glutaraldehyde in PBS at 4 °C for 20 min, followed by post-fixation in 1% osmium tetroxide for 30 min. Dehydration was performed using a series of ethanol concentrations (10 min incubation each in 50%, 60%, 70%, 80%, 90%, 95%, and 100% ethanol), after which the samples were air dried. The specimens were sputter-coated with platinum and examined by JEOL JSM-6500 TFE-SEM at an accelerating voltage of 5 kiloelectron volts (keV). The surface area of the cells grown on nanopores was quantified and compared to the surface area of cells grown on a flat surface using the ImageJ software package (NIH) to trace the cytoplasmic borders of the cells. SEM images of six different substrate fields were measured per sample, and three separate samples were measured for each nanopore surface.

2.5. Measurement of cell number by cell density

Cells were double stained using 4′,6-diamidino-2-phenylindole (DAPI) and phalloidin. NIH-3T3 fibroblasts were harvested and fixed using 4% paraformaldehyde diluted in PBS for 30 min, followed by three washes in PBS. Cell membranes were permeabilised during a 10 min incubation in 0.1% Triton X-100, followed by three PBS washes. MG63 cells were incubated with phalloidin and nuclei counterstained with DAPI for 15 min at room temperature. The samples were mounted and imaged using a Leica TCS SP2 confocal microscope. The cell number was counted using the ImageJ software package and expressed in terms of cell

Table 1
Gene names and sequence primers for real-time PCR.

Gene	Forward sequence	Reverse sequence
GAPDH	tcttcaccaccatggagaagg	ctcactggcatgaccttc
β1-integrin	gaggttcaatttgaaattagc	ggctctgcactgaacacattc
β2-integrin	aggagcatcgctaatcctga	ccagactcggtgatctcgtt
β3-integrin	ggacatctactacttgatgg	accgtgtctccaatcttgag
β4-integrin	agggaggctggctttcaatgtagt	ttcaccaggtgctcagtgtcatca
β5-integrin	tatgcactagtggaagtgcc	ccctcacacttcctctgacc
β6-integrin	tctgacattgttcagattgc	acttccagttccacctcaga
β7-integrin	agtgtgcgactgtaactgtggtga	actctgcacaatccctgtactgct
β8-integrin	caaaggacagtgtgcggaag	gttgacacagtgctgtgctg
α1-integrin	cgatgacgctctgccaaact	ccgaagttctggcattggga
α2-integrin	gcaccacattagcatacaga	ggcatcatacaggagaggaa
α3-integrin	gtctggaaaccttgtcaaccc	caaccacagctcaatctcagc
α4-integrin	cccaggctacatcgttttgt	ccatgctaatcccagtgtt
α5-integrin	ctgcagctgcatttccgagtctgg	gaagccgagcttgtagaggacgta
α6-integrin	tggaggtacagttgttggtgagca	aaacaccgtcactcgaacctgagt
α7-integrin	ccaggacctggccatccgtg	ctatccttgcgcagaatgac
α8-integrin	gcccagcttctgctgcaccg	cccaaggtcacacaccacca
α9-integrin	cctaacgttgcactgcaacc	agcagaaaaatgaggatcccc
α10-integrin	tggagtctctctccatcc	tcgatgaacagtcttcctaccagc
α11-integrin	ccgccttcctctgcttcataccca	gccgcctctcctcgttcacacacact
αIIb-integrin	tggtggtggcagcagaagaa	gtagggaggagacgttgaac
αD-integrin	tggatctcgactcgtggtgg	cactttttcgggccccattc
αE-integrin	ggacgatcaagcaacatcaa	ggaaccgtgctcattaaagg
αL-integrin	ttgagggcacaaacagacag	tcatccaggccacagtgtaa
αM-integrin	cagatcaacaatgtgaccgtatgg	catcatgtccttgtactgccgc
αV-integrin	gtcttatacagagccagacccg	cttcacagtcagtgtcagaggg
αX-integrin	acacagtgtgctccagtatga	gcccagggatatgttcacagc

Download English Version:

https://daneshyari.com/en/article/10229265

Download Persian Version:

https://daneshyari.com/article/10229265

Daneshyari.com